GEOPHYSICAL RESEARCH LETTERS, VOL. 35, L17603, doi:10.1029/2008GL035129, 2008

Relationship between typhoon activity and upper ocean heat content

A. Wada[1] and J. C. L. Chan[2]

Received 25 June 2008; revised 4 August 2008; accepted 14 August 2008; published 13 September 2008.

[1] A 44-year mean distribution of tropical cyclone heat potential (TCHP), a measure of the oceanic heat content from the surface to the 26°C-isotherm depth, shows that TCHP is locally high in the western North Pacific (WNP). TCHP varies on interannual time scales and has a relationship with tropical cyclone (TC) activity. The third mode of an empirical orthogonal function analysis of TCHP shows that an increase in the total number of TCs is accompanied with a warm central Pacific and cool WNP. Negative TCHP anomalies in the WNP suggest that an increase in total number of TCs results in cooling due to their passages. On the other hand, the first mode shows that the number of super typhoons increases in mature El Niño years. An increase in accumulated TCHP is related to the increase in the number of super typhoons due to long duration. **Citation:** Wada, A., and J. C. L. Chan (2008), Relationship between typhoon activity and upper ocean heat content, *Geophys. Res. Lett.*, *35*, L17603, doi:10.1029/2008GL035129.

1. Introduction

[2] Recent studies suggested a large increase in the number and proportion of intense tropical cyclones (TCs) reaching categories 4 and 5 on the Saffir-Simpson scale and that the trend was due to both longer storm lifetimes and greater storm intensities associated with global warming in the North Atlantic and North Pacific [e.g., *Webster et al.*, 2005; *Emanuel*, 2005]. A strong El Niño-Southern Oscillation (ENSO) signal is related to the mean location of TC formation [*Chia and Ropelewski*, 2002], its mean life span, mean number of TC occurrence [*Wang and Chan*, 2002; *Camargo and Sobel*, 2005], TC landfalling activity [*Wu et al.*, 2004] and mean recurvature area of TC track [*Camargo et al.*, 2007a]. The index of ENSO has been used as one of predictors for seasonal forecasts of TC activity in various basins [*Chan et al.*, 1998, 2001; *Camargo et al.*, 2007b]. However, in the western North Pacific (WNP), whether variations in TC activity (TC numbers and intensity) are a part of the large interdecadal variability [*Chan*, 2006] or due to an increase in sea surface temperature (SST) [*Webster et al.*, 2006] has not been resolved.

[3] Recently, in addition to SST, tropical cyclone heat potential (TCHP) [*Leipper and Volgenau*, 1972] has been studied in regard to its possible relation with TC intensity [e.g., *Goni and Trinanes*, 2003]. In fact, TCHP is correlated with mature TC intensity and its variation [*Wada and Usui*, 2007]. In that sense, TCHP can be regarded as a factor that explains TC intensity. In general, the passage of a TC results in sea-surface cooling, decrease in sea surface heat flux and suppression of the development of TCs and thus TCHP decreases. Quite a few studies have supported such a locally-transient TC-ocean interaction. However, TC-ocean interaction on climate scales, particularly features of TCHP, has not been known due to the unavailability of a long historical oceanic dataset. A further question is whether or not warming in a basin scale during the last 50 years [*Levitus et al.*, 2005a] has affected TC activity. This paper therefore examines the climatological features of TCHP and investigates its relationship with TC activity in the WNP.

2. Data and Methods

2.1. Oceanic Reanalysis Data

[4] We use a monthly oceanic reanalysis dataset with a grid resolution of 0.5° latitude × 0.5° longitude from 1961 to 2004. The dataset is calculated by the North Pacific version of the Japan Meteorological Agency/Meteorological Research Institute Multivariate Ocean Variational Estimation system (MOVE) [*Usui et al.*, 2006]. For oceanic assimilation by the MOVE system, in situ observations from ships, buoys, and Argo floats are obtained from the web sites of the World Ocean Database 2001 (http://www.nodc.noaa.gov/OC5/WOA01/1d_woa01.html) and the Global Temperature-Salinity Profile Program (http://www.nodc.noaa.gov/GTSPP/gtspp-home.html). In addition, satellite altimeter data have been used for oceanic assimilation by the MOVE system since 1993. The assimilation system includes an ocean general circulation model [*Ishikawa et al.*, 2005], which is driven by the National Center for Environmental Prediction-National Center for Atmospheric Research atmospheric reanalysis data [*Kalnay et al.*, 1996].

2.2. Tropical Cyclone Heat Potential

[5] TCHP is defined as [*Leipper and Volgenau*, 1972]:

$$Q_{TCHP} = \sum_{h=0}^{H} \rho_h C_p (T_h - 26) \Delta Z_h, \quad (1)$$

where ρ_h is the density of the sea water at each layer, C_p the specific heat capacity at constant pressure, T_h the sea water temperature (°C) at each layer and ΔZ_h the thickness at each layer, H the vertical level of depth corresponding to the isotherm of 26°C (hereafter Z26) and h the variable number of vertical level based on the configuration of MOVE dataset. When T_h is below 26°C, TCHP at the layer is assumed to be zero.

[1] Meteorological Research Institute Japan Meteorological Agency, Tsukuba, Japan.
[2] Guy Carpenter Asia-Pacific Climate Impact Centre, City University of Hong Kong, Kowloon, Hong Kong.

0094-8276/08/2008GL035129$05.00

2.3. Calculation of the Ratio of Interannual to Seasonal TCHP Amplitude

[6] To understand the relative magnitudes of TCHP variations between seasonal and interannual time scales, the ratio (r) of the interannual variations of TCHP to those on a seasonal scale is introduced as

$$r = \frac{\sqrt{\overline{\left(H_{y,m} - \overline{H_m}\right)^2}}}{\sqrt{\overline{\left(H_{y,m} - \overline{H}\right)^2}}}, \quad (2)$$

where $H_{y,m}$ is the raw data of TCHP in the yth year and the mth month. $\overline{H_m}$ the monthly mean of TCHP of the mth month over 44 years from 1961 to 2004, and $\overline{H}$ the 44-year mean TCHP. The overbar shows the mean value of each summation for each year, month or both.

2.4. TC Best-Track Data

[7] Here we use the Joint Typhoon Warming Center (JTWC) best track data (http://metocph.nmci.navy.mil/jtwc/best_tracks/wpindex.html) from 1961 to 2004 to obtain the 6-hour best-track positions of TCs and their maximum sustained wind speeds over the WNP. We define TC-related parameters in the following: TC duration day (TCDAY) is a period during which the maximum wind speed is $\geq$ 34 knots. The period of typhoon (maximum wind speed $\geq$ 64 knots) is called typhoon-duration day (TYDAY). The period of super-typhoon (maximum wind speed $\geq$ 115 and Saffir-Simpson categories 4 and 5) is called super-typhoon-duration day (STYDAY). Each number of TC, typhoon, and super-typhoon is called TCNUM, TYNUM, and STYNUM, respectively.

[8] Accumulated cyclone energy [*Bell et al.*, 2000] is calculated by summing the squares of the estimated maximum sustained wind speeds of every active tropical storm (maximum wind speed $\geq$ 34 knots: ACE), every active tropical storm until first reaching category 4 (maximum wind speed $\leq$ 115 knots: ACE4), and every active super-typhoon (ACES), at six-hour intervals. The unit of ACE is 10^4 kt^2.

[9] Power dissipation index [*Emanuel*, 2005] is calculated by summing the cubes of the estimated maximum sustained wind speeds of every active tropical storm (maximum wind speed $\geq$ 34 knots: PDI), every active tropical storm until first reaching category 4 (the maximum wind speed $\leq$ 115 knots: PDI4), and every active super-typhoon (PDIS), at six-hour intervals. The unit of PDI is 10^6 kt^3.

3. Results

3.1. Climatological Distribution of TCHP

[10] While seasonal variations of TCHP are dominant particularly in the low-latitude WNP (small value of r), the ratio of interannual to seasonal TCHP variations is locally high around 10°N, 130°–140°E ('A' in Figure 1a) like a footprint over the warm ocean. The climatological distribution of TCHP over the Pacific shows two high TCHP areas: one around the tropical central Pacific and the other in the WNP ('B' and 'C' in Figure 1b respectively). TCs are generated around the high TCHP region in the WNP (Figure 1c). The ratio of interannual to seasonal Z26 variations is locally high around 10°N, 130°–140°E ('D' in Figure 1d). East of the Philippines, this ratio is locally high where Z26 is relatively shallow (Figure 1e), while Z26 is relatively deep around the tropical central Pacific ('E' in Figure 1e) and in the WNP ('F' in Figure 1e). The 'footprint' region found in both TCHP and Z26 distributions is located in south of '*the preferred region of rapid intensification* (8°N–20°N, 125°E–155°E, square box drawn in Figure 1f)' [*Wang and Zhou*, 2008]. Super typhoons at first reaching category 4 congregate where TCHP and Z26 gradients are steep in the WNP (Figure 1f).

3.2. EOF Analysis

[11] To examine representative patterns of interannual upper-ocean variations, we need to exclude the intraseasonal variations from the raw monthly TCHP data. Here an empirical orthogonal function (EOF) analysis of 12-month running mean monthly TCHP anomaly dataset is made. Three EOFs account for 38.5%, 23.0% and 11.8% of the total variance (Table 1). All these EOFs are clearly distinct from one another based on the test proposed by *North et al.* [1982].

[12] The spatial pattern of the first mode features an east-west pattern with opposite signs, which apparently represents the ENSO signal (Figure 2a). In fact, the normalized amplitude of this mode is well correlated with the SST anomalies in the NINO3 region (http://www.data.jma.go.jp/gmd/cpd/data/elnino/index/nino3anm.html) (5°N–5°S, 150–90°W) with a correlation coefficient of 0.82. The correlation is significant at the 99% significant level based on the t-test (Table 1). The second mode features a pattern flanked by a pattern of the opposite sign in the equatorial eastern Pacific (Figure 2b), which is similar to a unique tripolar pattern called 'El Niño Modoki' ("Modoki" is a classical Japanese word, which means "a similar but different things" [*Ashok et al.*, 2007].). The El Niño Modoki involves ocean-atmosphere coupled processes which include a unique tripolar sea level pressure pattern during the evolution [*Ashok et al.*, 2007]. These first two EOF modes are often analyzed [e.g., *Levitus et al.*, 2005b]. Although a downward trend is found in the second EOF mode (Figure 2b), neither the slope nor the intercept is significant based on the t-test. Therefore, we cannot clarify the role of the warming in TC activity using the present TCHP dataset.

[13] A downward trend is also found in the third EOF mode (Figure 2c) although neither the slope nor the intercept is significant, either. However, unlike the downward trend in the second mode, the trend in the third mode is strongly affected by the normalized amplitude in 1983 and 1998 (gray masks in Figure 2). In 1983 and 1998, TCNUM and TYNUM are actually low (not shown). Even though the values of slope and intercept are insignificant, the variations of the third mode in 1983 and 1998 differentiate this mode from the other EOF modes.

[14] In fact, the third mode shown in Figure 2c has never been discussed in previous studies. The spatial pattern of this mode has the same sign in the WNP and eastern equatorial Pacific and an opposite sign in the central Pacific region. The normalized amplitude of this mode is correlated with TCNUM and TYNUM (Table 1). These correlations are significant at the 99% significant level based on the t-test but the amplitudes are not significantly correlated with

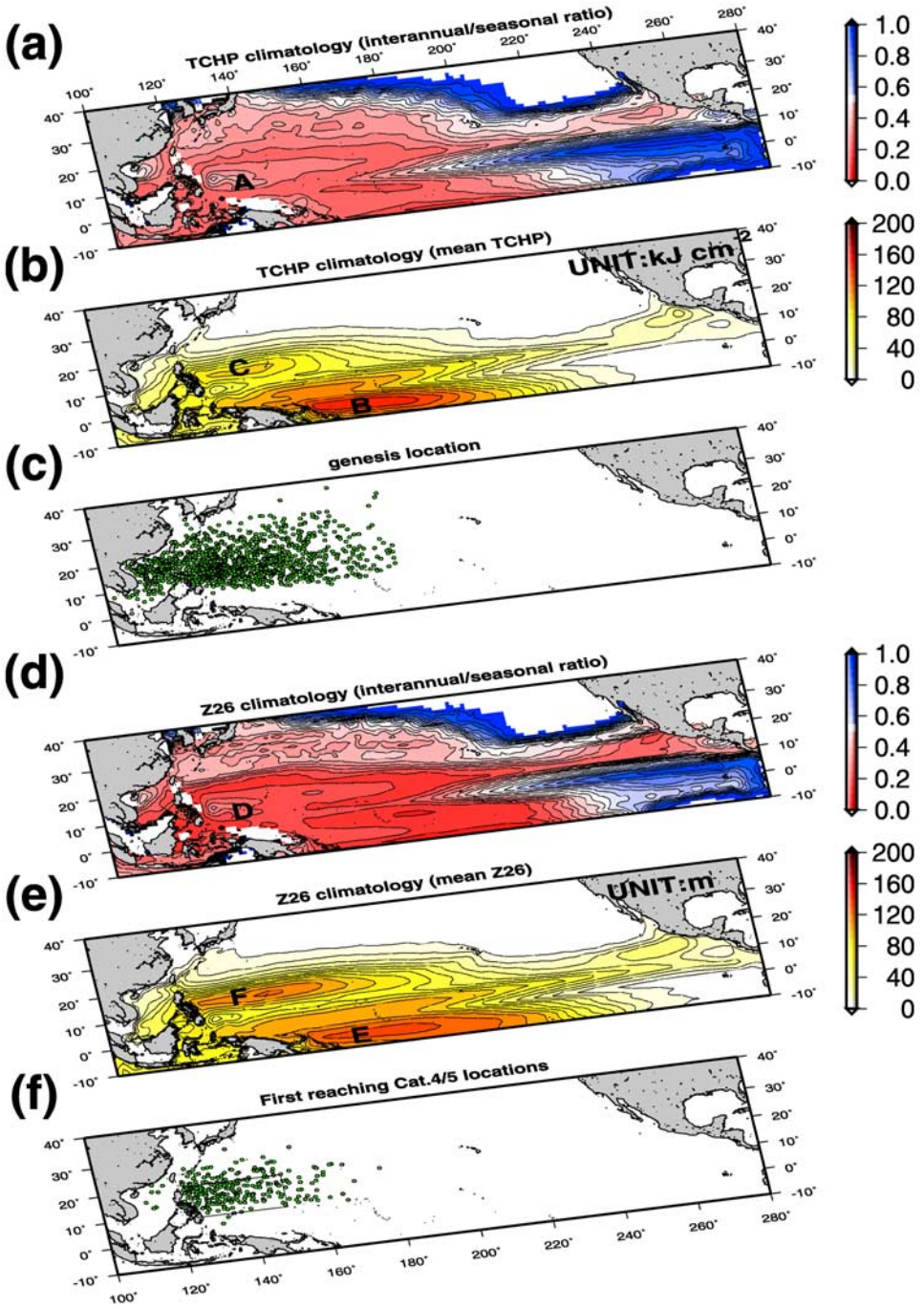

Figure 1. Horizontal distributions of (a) the ratio of root mean square of TCHP anomaly deviated from monthly mean TCHP for 44 years to that of the anomaly deviated from annual mean tropical cyclone heat potential for 44 years, (b) TCHP averaged from 1961 to 2004, (c) genesis locations from JTWC best-track data, (d) as in Figure 1a except for Z26, (e) as in Figure 1b except for Z26, and (f) as in Figure 1c except for the locations of TCs first reaching an intensity corresponding to category 4 on the Saffir-Simpson scale. Labels A–F show high ratio of TCHP (A), high TCHPs (B, C), high ratio of Z26 (D) and high Z26s (E,F). A square drawn in Figure 1f shows the area of rapid intensification [*Wang and Zhou*, 2008].

the SST anomalies in the NINO3 region. This result implies that the occurrence of central Pacific warming, WNP cooling and equatorial eastern Pacific cooling is independent of ENSO and is accompanied with an increase in the total number of TCs. This suggests a locally transient TC-ocean interaction caused by the passage of TCs. The WNP cooling pattern is probably caused by the superposition of frequent passage of TCs.

[15] From a lag-correlation analysis of normalized amplitude between the first and third modes, the third mode precedes the first mode at a lag of 12 months. The value of correlation 0.42 is significant at the 99% significant level

Table 1. Correlation Coefficients Between Normalized Loading Amplitudes of the First Three EOF Modes and Index Associated With ENSO (NINO3) and TC Activity[a]

	NINO3	TCNUM	TYNUM	STYNUM	TCDAY	TYDAY	STYDAY	ACE	ACE4	ACES	PDI	PDI4	PDIS
EOF1(38.5%)	***0.82***	0.02	0.20	*0.36*	***0.47***	***0.43***	***0.40***	***0.46***	***0.40***	*0.36*	***0.43***	***0.39***	*0.34*
EOF2(23.0%)	0.20	0.04	0.04	−0.09	−0.05	−0.07	−0.14	−0.09	−0.07	−0.10	−0.09	−0.09	−0.07
EOF3(11.8%)	−0.06	***0.45***	***0.55***	0.29	***0.40***	*0.35*	0.27	***0.41***	***0.45***	0.28	***0.39***	***0.47***	0.29

[a]Bold font shows that the correlation is significant at the 99% significant level and italic font shows that the correlation is significant at the 95% significant level.

based on the *t*-test. This suggests that TC activity in the WNP may play an active role in the development of ENSO events as suggested by *Sobel and Camargo* [2005].

3.3. EOF Modes and TC Activity

[16] Table 1 also shows that STYNUM has a positive and significant correlation with the first EOF (the El Niño mode), but no relationship exists between the EOF third mode and STYNUM. Therefore, the relationship between TC activity and climatological TCHP is different during the lifecycle of a TC. The difference in correlations and their significance is also found in duration, ACE and PDI. The third mode is significantly correlated with TCDAY, TYDAY, ACE, ACE4, PDI and PDI4 (Table 1). The first mode is, in addition, correlated with STYDAY, ACES and PDIS at the 95% significant level based on the *t*-test (Table 1). The increase in TCDAY, ACE and PDI during the El Niño is consistent with the previous studies [*Camargo and Sobel*, 2005; *Chan*, 2007].

[17] The relationship between the ENSO and super-typhoon is explored from the perspective of TCHP variation. The years of El Niño (1963, 1965, 1969, 1972, 1982, 1983, 1987, 1991, 1992, 1997, and 2002) and La Niña (1964, 1971, 1975, 1985, 1988, 1989, 1999, 2000) events are determined using the criterion of an annual average of NINO3 SST anomalies being higher than 0.5°C (−0.5°C). Climatologically, super-typhoons are generated from May to December with a peak from August to October. A 44-year average of TCHP at a TC position on the track of super-typhoon is 77.9 kJ cm^{-2}, while an average of TCHP during the El Niño (La Niña) events is 74.4 kJ cm^{-2} (78.4 kJ cm^{-2}). During an El Niño (a La Niña) year, the averages of STYDAY [40.0 days (19.0 days)], ACES [$116.8 \cdot 10^4$ kt^2 ($94.7 \cdot 10^4$ kt^2)] and PDIS [$112.1 \cdot 10^6$ kt^3 ($81.0 \cdot 10^6$ kt^3)] are larger (smaller) than the 44-year averages of STYDAY [29.4 days], ACES [$108.5 \cdot 10^4$ kt^2] and PDIS [$96.7 \cdot 10^6$ kt^3]. This result suggests that formation of super-typhoon is not directly related to TCHP at a TC position.

[18] Now accumulated TCHP [e.g., *Wada and Usui*, 2007] is roughly defined as the product of TCHP and STYDAY. The product in the El Niño (La Niña) event is 3.0 MJ cm^{-2}·day (1.5 MJ cm^{-2}·day), while a 44-year average product is 2.3 MJ cm^{-2}·day. Therefore, a long duration of TC over the warm ocean is essential for super-typhoon formation due to an increase in ATCHP, consistent with the conclusion of *Chan* [2008]. In fact, specific track types related to ENSO [*Camargo et al.*, 2007a] and southeastward shift of TC genesis location cause long duration and thus an increase in ATCHP.

3.4. Cooling Effect

[19] WNP cooling (warming) around 8–20°N, 120–150°E is possibly related to the subsequent (deficient) passage of TCs. In fact, TCHP anomalies are positive (negative) when TYNUM decreases (increases). Around 8–20°N, 120–150°E the upper ocean loses TCHP due to enhanced TC activity (see auxiliary material Figure S1[1]). Assuming that the difference in TCHP anomaly between large TCNUM and small one is nearly 4 kJ cm^{-2}, the difference in Z26 nearly 0.32 cm and density 1.023 g cm^{-3}, the difference in temperature derived from the equation (1) is nearly 2.9°C. Indeed, the amplitude of Z26 variation is diminutive compared with that of TCHP (not shown). Because of small percentage of variance in the third mode (11.8%) compared with that in the first and second modes, a decrease in SST due to TC activity is estimated to be at most nearly 0.34°C.

4. Discussion

[20] The TC activity-related pattern of TCHP has never been addressed in the previous studies. Here we show that the EOF third mode of TCHP represents the occurrence of oceanic response to subsequent passages of TCs. However, the amplitude of rapid sea-surface cooling caused by a passage of a TC is not realistically reproduced in the present MOVE system [*Wada and Usui*, 2007] due to its coarse horizontal resolution, uncertainty of atmospheric forcing, deficient observations and problems of assimilation scheme. If atmospheric reanalysis data is capable of resolving realistic amplitude of TC wind, the amount of variance explained by the EOF third mode will probably increase. However, an improvement of best-track data [*Knaff and Zehr*, 2007] and further evaluation of oceanic reanalysis data, for example reliability of trends, are needed to develop the present study even if the historical oceanic reanalysis dataset actually provides us with the information of historical TC activities over the ocean.

[21] The WNP cooling associated with TC activity is mainly produced due to strong-wind-induced vertical turbulent mixing and upwelling. The oceanic response to TCs is possibly related to formation of the steep gradients north of the maximum area of TCHP and Z26 (Figure 1). On the other hand, at a footprint region, interannual variations of TCHP are dominant south of high TCHP area where oceanic responses to TCs easily occur due to relatively shallow Z26. The interannual variation at the footprint region may be related to large-scale atmospheric circulations such as the monsoon trough and the Madden-Julian Oscillation [*Madden and Julian*, 1972] that are considered to result in the genesis and development of TCs in the WNP.

[1]Auxiliary materials are available in the HTML. doi:10.1029/2008GL035129.

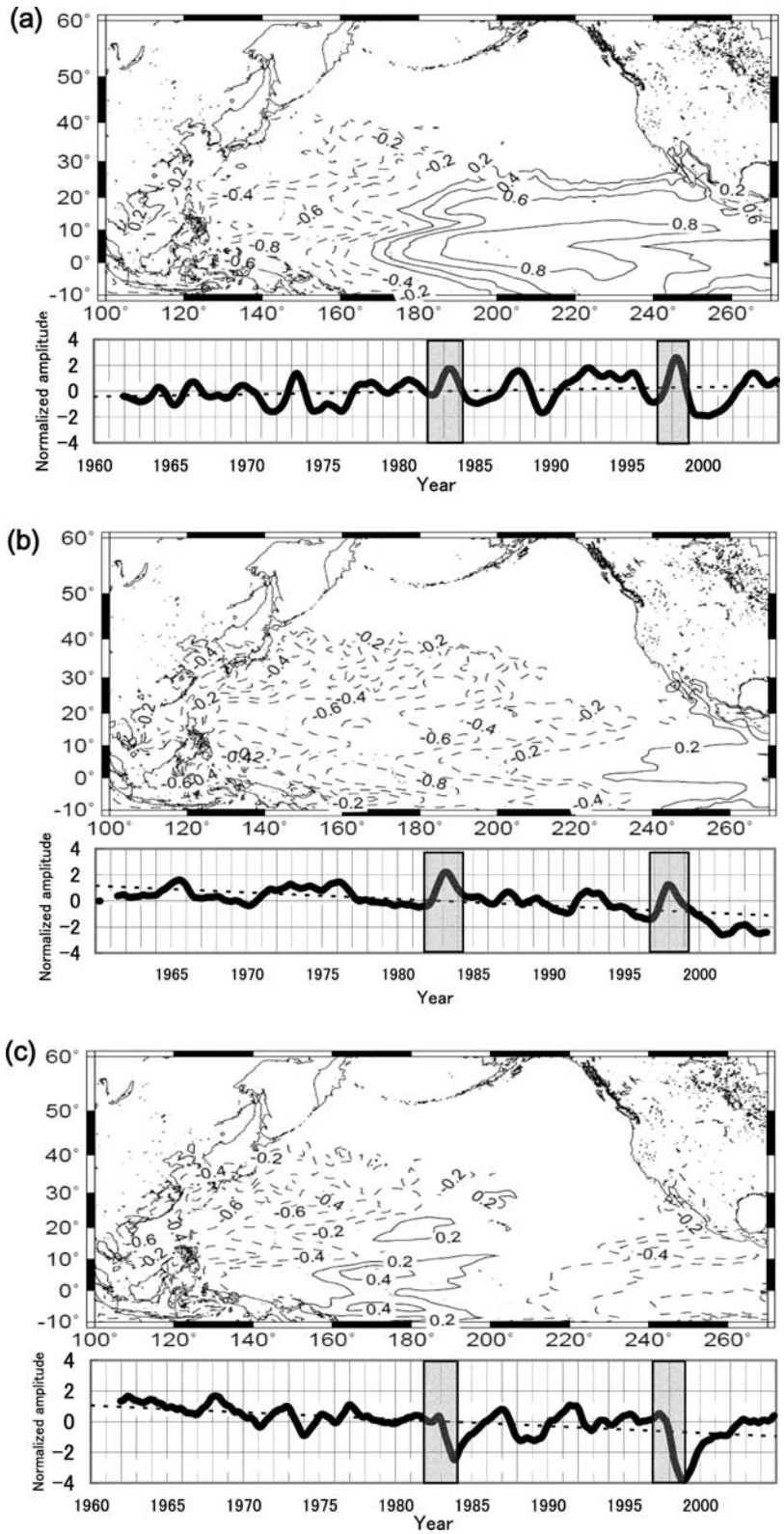

Figure 2. Upper panels show spatial patterns derived from the EOF analysis for TCHP and lower panels show time series of 12-months running mean of normalized loading amplitude: (a) in the first mode, (b) in the second mode, and (c) in the third mode. In the upper panels, solid lines indicate positive correlation, and dashed lines indicate negative correlation. In the lower panels, solid lines show time series of 12-months running mean of normalized loading amplitude and dashed lines show their trend. The years 1983 and 1998 are indicated by grey-shaded boxes.

[22] **Acknowledgments.** The authors would like to thank the reviewers for providing us useful comments to improve an early draft of the paper. The first author thanks Mr. S. Matsumoto for providing the oceanic reanalysis dataset used in the present study and for his useful comments. The work of the second author was done as a Visiting Professor at the Center for Climate Systems Research (CCSR) of the University of Tokyo. He would like to thank CCSR for supporting his visit. The Generic Mapping Tools (GMT) was used to draw panels.

References

Ashok, K., S. K. Behera, S. A. Rao, H. Weng, and T. Yamagata (2007), El Niño Modoki and its possible teleconnection, *J. Geophys. Res.*, *112*, C11007, doi:10.1029/2006JC003798.

Bell, G. D., et al. (2000), Climate assessment for 1999, *Bull. Am. Meteorol. Soc.*, *81*, S1–S50, doi:10.1175/1520-0477(1999)080<1040:CAF>2.0.CO;2.

Camargo, S. J., and A. H. Sobel (2005), Western North Pacific tropical cyclone intensity and ENSO, *J. Clim.*, *18*, 2996–3006, doi:10.1175/JCLI3457.1.

Camargo, S. J., A. W. Robertson, S. J. Gaffney, P. Smyth, and M. Ghil (2007a), Cluster analysis of typhoon tracks. Part II: Large-scale circulation and ENSO, *J. Clim.*, *20*, 3654–3676, doi:10.1175/JCLI4203.1.

Camargo, S. J., A. G. Barnston, P. J. Klotzbach, and C. W. Landsea (2007b), Seasonal tropical cyclone forecasts, *WMO Bull.*, *56*, 297–309.

Chan, J. C. L. (2006), Comment on "Changes in tropical cyclone number, duration, and intensity in a warming environment", *Science*, *311*(5768), 1713, doi:10.1126/science.1121522.

Chan, J. C. L. (2007), Interannual variations of intense typhoon activity, *Tellus, Ser. A*, *59*, 455–460, doi:10.1111/j.1600-0870.2007.00241.x.

Chan, J. C. L. (2008), Decadal variations of intense typhoon occurrence in the western North Pacific, *Proc. R. Soc. London, Ser. A*, *464*, 249–272, doi:10.1098/rspa.2007.0183.

Chan, J. C. L., J. E. Shi, and C. M. Lam (1998), Seasonal forecasting of tropical cyclone activity over the western North Pacific and the South China Sea, *Weather Forecast.*, *13*, 997–1004, doi:10.1175/1520-0434(1998)013<0997:SFOTCA>2.0.CO;2.

Chan, J. C. L., J. E. Shi, and K. S. Liu (2001), Improvements in the seasonal forecasting of tropical cyclone activity over the western North Pacific, *Weather Forecast.*, *16*, 491–498, doi:10.1175/1520-0434(2001)016<0491:IITSFO>2.0.CO;2.

Chia, H. H., and C. F. Ropelewski (2002), The interannual variability in the genesis location of tropical cyclones in the Northwest Pacific, *J. Clim.*, *15*, 2934–2944, doi:10.1175/1520-0442(2002)015<2934:TIVITG>2.0.CO;2.

Emanuel, K. A. (2005), Increasing destructiveness of tropical cyclones over the past 30 years, *Nature*, *436*, 686–688, doi:10.1038/nature03906.

Goni, G. J., and J. A. Trinanes (2003), Ocean thermal structure monitoring could aid in the intensity forecast of tropical cyclones, *Eos Trans. AGU*, *84*, 577.

Ishikawa, I., H. Tsujino, M. Hirabara, H. Nakano, T. Yasuda, and H. Ishizaki (2005), *Meteorological Research Institute Community Ocean Model (MRI.COM) Manual* (in Japanese), *Tech. Rep. Meteorol. Res. Inst. 47*, 189 pp., Meteorol. Res. Inst., Tsukuba, Japan.

Kalnay, E., M. Kanamitsu, R. Kistler, W. Collins, D. Deaven, L. Gandin, M. Iredell, S. Saha, G. White, and J. Woollen (1996), The NCEP/NCAR 40-year reanalysis project, *Bull. Am. Meteorol. Soc.*, *77*, 437–471, doi:10.1175/1520-0477(1996)077<0437:TNYRP>2.0.CO;2.

Knaff, J. A., and R. M. Zehr (2007), Reexamination of tropical cyclone wind-pressure relationships, *Weather Forecast.*, *22*, 71–88, doi:10.1175/WAF965.1.

Leipper, D. F., and D. Volgenau (1972), Hurricane heat potential of the Gulf of Mexico, *J. Phys. Oceanogr.*, *2*, 218–224.

Levitus, S., J. Antonov, and T. Boyer (2005a), Warming of the world ocean, 1955–2003, *Geophys. Res. Lett.*, *32*, L02604, doi:10.1029/2004GL021592.

Levitus, S., J. I. Antonov, T. P. Boyer, H. E. Garcia, and R. A. Locarnini (2005b), EOF analysis of upper ocean heat content, 1956–2003, *Geophys. Res. Lett.*, *32*, L18607, doi:10.1029/2005GL023606.

Madden, R. A., and P. R. Julian (1972), Description of global-scale circulation cells in the tropics with a 40–50 day period, *J. Atmos. Sci.*, *29*, 1109–1123.

North, G. R., T. L. Bell, R. F. Cahalan, and F. J. Moeng (1982), Sampling errors in the estimation of empirical orthogonal functions, *Mon. Weather Rev.*, *110*, 699–706.

Sobel, A. H., and J. Camargo (2005), Influence of western North Pacific tropical cyclones on their large-scale environment, *J. Atmos. Sci.*, *62*, 3396–3407, doi:10.1175/JAS3539.1.

Usui, N., S. Ishizaki, Y. Fujii, H. Tsujino, T. Yasuda, and M. Kamachi (2006), Meteorological Research Institute multivariate ocean variational estimation (MOVE) system: Some early results, *Adv. Space Res.*, *37*(4), 806–822.

Wada, A., and N. Usui (2007), Importance of tropical cyclone heat potential for tropical cyclone intensity and intensification in the Western North Pacific, *J. Oceanogr.*, *63*, 427–447.

Wang, B., and J. C. L. Chan (2002), How strong ENSO events affect tropical storm activity over the western North Pacific, *J. Clim.*, *15*, 1643–1658, doi:10.1175/1520-0442(2002)015<1643:HSEEAT>2.0.CO;2.

Wang, B., and X. Zhou (2008), Climate variation and prediction of rapid intensification in tropical cyclones in the western North Pacific, *Meteorol. Atmos. Phys.*, *99*, 1–16, doi:10.1007/s00703-006-0238-z.

Webster, P. J., G. J. Holland, J. A. Curry, and H.-R. Chang (2005), Changes in tropical cyclone number, duration, and intensity in a warming environment, *Science*, *309*(5742), 1844–1846, doi:10.1126/science.1116448.

Webster, P. J., J. A. Curry, J. Liu, and G. J. Holland (2006), Response to comment on "Changes in tropical cyclone number, duration, and intensity in a warming environment", *Science*, *311*(5768), 1713, doi:10.1126/science.1121564.

Wu, M. C., W. L. Chang, and W. M. Leung (2004), Impacts of El Niño-Southern Oscillation events on tropical cyclone landfalling activity in the western North Pacific, *J. Clim.*, *17*, 1419–1428, doi:10.1175/1520-0442(2004)017<1419:IOENOE>2.0.CO;2.

J. C. L. Chan, Guy Carpenter Asia-Pacific Climate Impact Centre, City University of Hong Kong, Kowloon, Hong Kong.

A. Wada, Meteorological Research Institute Japan Meteorological Agency, 1-1 Nagamine, Tsukuba, Ibaraki, 305-0052, Japan. (awada@mri-jma.go.jp)